

We are IntechOpen, the world's leading publisher of Open Access books Built by scientists, for scientists

6,900

Open access books available

186,000

International authors and editors

200M

Downloads

Our authors are among the

154

Countries delivered to

TOP 1%

most cited scientists

12.2%

Contributors from top 500 universities



WEB OF SCIENCE™

Selection of our books indexed in the Book Citation Index
in Web of Science™ Core Collection (BKCI)

Interested in publishing with us?
Contact book.department@intechopen.com

Numbers displayed above are based on latest data collected.
For more information visit www.intechopen.com



Amorphous Calcium Phosphate as Bioactive Filler in Polymeric Dental Composites

Diane R. Bienek, Anthony A. Giuseppetti and Drago Skrtic

Abstract

As biocompatible and osteo-inductive precursor to biological apatite formation, amorphous calcium phosphate (ACP) resorbs at the rate that closely coincides with the rate of new bone formation and is more osteo-conductive than its crystalline counterpart. In addition, in the oral environment, ACP intrinsically provides a protracted supply of the remineralizing calcium and phosphate ions needed for regeneration of mineral lost to tooth decay. These features make ACP composites a strong remineralizing tool at the site of caries attack. Our group has been on the forefront of the research on bioactive, remineralizing, polymeric ACP-based dental materials for over two decades. This entry describes methods for filler, polymer, and composite fabrication and a battery of physicochemical and biological tests involved in evaluation of ACP-based restoratives. Also presented is our most recent design of ACP remineralizing composites with added antimicrobial capability that shows promise for extended dental and, potentially, wider biomedical applications.

Keywords: amorphous calcium phosphate, bioactivity, dental composite, dental resin, remineralization

1. Introduction

Due to their abundance in nature as phosphate minerals and their existence in living organisms, calcium phosphates (CaPs) are of special significance to humans. CaPs are involved in normal (bones, teeth, antlers) as well as pathological (calcification/mineral deposition in soft tissues) mineralization. Both normal and pathological calcifications represent *in vivo* crystallization. In contrast, dental caries and osteoporosis are manifestations of *in vivo* dissolution where less soluble CaPs are being replaced by the more soluble ones. The extensive overviews of the current knowledge on CaP structures, properties, and biomedical and dental importance are provided in Refs. [1–4].

Amorphous calcium phosphates (ACPs) are unique members of CaP family with glass-like physical properties and variable chemistry [5]. Evidence of ACPs being an integral mineral component of bones and teeth is, however, ambiguous [6, 7]. Consequently, ACPs are considered the transient precursors in biomineralization [8–11] with the majority of information on their possible roles in biomineralization originating from the synthetic and/or *in vitro* studies [12].

The use of CaPs in dentistry is roughly a century old with the first scientific article published in 1925 [3]. Majority of the literature on dental use of CaPs focuses on crystalline CaPs. Today, two ACP-based remineralization systems have been commercialized as a toothpaste: a casein phosphopeptide-stabilized ACP and an unstabilized ACP. Other ACP applications include various biocompatible formulations where ACP acts as anticariogenic, remineralizing agent (polymeric composites, chewing gums, sugar confections, bleaching gels, and/or mouth rinses).

In this chapter, we present an overview of our group's up-to-date work on ACP-based dental composites with the emphasis on fabrication and characterization of ACP filler, fine-tuning of polymer phase, and physicochemical, mechanical, and biological evaluation of the ensuing polymeric ACP composites. Attention is also given to our most recent efforts to develop bioactive composites with both remineralizing and antimicrobial (AM) capabilities.

2. ACP-based polymeric dental composites

The approaches to synthesize ACP include precipitation from supersaturated calcium and phosphate solutions (wet synthesis), spray drying of acidified aqueous solutions of soluble CaPs, precipitation from nonaqueous solutions and solvents (sol-gel technique), and dry chemical techniques (mechanochemical methods, high-energy processing at elevated temperatures). Morphology, chemical composition, atomic structure, thermal properties, mechanical properties, and kinetics of ACP's transformation into crystalline CaPs depend on the preparation method [5]. ACPs fabricated by wet chemical method typically have a relatively constant chemical composition, suggesting the existence of well-defined structural units/clusters [12, 13]. ACPs are thermodynamically unstable in solutions and convert spontaneously into crystalline CaPs, predominantly apatite. As result of ACP to apatite transformation, both crystallinity and Ca/P ratios of the solid increase with time. The release of remineralizing ions that accompany ACP's transformation in solutions, coupled with their excellent biocompatibility and bioresorbability, makes ACP-based dental materials a powerful remineralizing tool. However, the unique benefit of ACP-based materials, i.e., their sustained remineralization capability, is compromised by the inherently low strength and toughness of ACP composites due to the uncontrolled agglomeration of ACP particles and enhanced water sorption (WS) on exposure to aqueous environment [14]. To overcome these deficiencies, we explored multiple approaches to reduce the heterogeneity of filler particle size distribution (PSD) and better control the stability of the ACP/resin interface. These attempts are described in Sections 2.1–2.3.

2.1 ACP filler: synthesis, characterization, and surface modification

ACPs utilized in our studies were synthesized according to the protocol originally proposed [15]. It was modified to include *ab initio* addition of cations or nonionic surfactants to Ca reactant and anionic surfactant or polymer to PO_4 reactant. In brief, ACP precipitated instantly upon mixing equal volumes of the reactant solutions {Ca reactant, 80 mmol/L $\text{Ca}(\text{NO}_3)_2$; PO_4 reactant, 54 mmol/L $\text{Na}_2\text{HPO}_4 + 2 \text{ mol}\% \text{Na}_4\text{P}_2\text{O}_7$ (to inhibit the precipitation of apatite simultaneously with ACP)} at 23°C and $\text{pH} \geq 8.5$. After filtering, solid was subsequently washed with ice-cold ammoniated water, then with acetone, freeze-dried, and lyophilized. Dry, as-synthesized ACP (as-ACP) was kept in dessicator under vacuum before being subjected to additional treatments: silanization [16], grinding [17], or mechanical milling [14]. Before being utilized for composite fabrication, ACPs were

characterized (validated) by multiple screenings. The amorphousness of the solids was confirmed by X-ray diffraction (XRD) analysis and Fourier-transform infrared (FTIR) spectroscopy. PSD of ACP dispersed in isopropanol was determined by laser light scattering, and their morphology/topology of gold-sputtered specimens was assessed by scanning electron microscopy (SEM). ACP's water content was measured by thermogravimetric analysis (TGA), and Ca/PO₄ ratio was calculated from atomic emission spectroscopy data obtained upon dissolving ACP powder in HCl. Typical XRD pattern, FTIR spectrum, and SEM image of ACP are presented in **Figure 1**. More detailed description of ACP preparatory protocols and filler's characterization/validation is provided [18]. The same reference is also a good source of information on methods and techniques utilized in preparation and evaluation of copolymers and composites and their physicochemical, mechanical, and biological assessments discussed in Sections 2.2 and 2.3.

Introducing additives during ACP synthesis and/or applying secondary treatments (**Table 1**) was expected to yield less clustered dry powders (more homogeneous and narrower PSD) and lead to better dispersion of ACP in the resin. Experimental details on surface modification protocols are provided in [16, 19]. More intimate ACP/resin contact is expected to enhance hydrolytic stability of ACP through lowering the WS, thus improving the mechanical performance of composites.

The coprecipitation of Ag and Fe phosphates and premature ACP to apatite conversion in the presence of Fe²⁺ and Fe³⁺ disqualified these cations from further evaluation. Results of PSD analysis and TGA results obtained with surface-modified ACPs and strength testing of model 2,2-bis[p-(2'-hydroxy-3'-methacryloxypropoxy) phenyl] propane (Bis-GMA)-based composites employing these fillers are summarized in **Figure 2**.

Regardless of the type of treatment, practically all ACPs preserved their heterogeneous PSDs. However, values of the median diameter (d_m), i.e., the midpoint of the volume size distribution, of Zn-ACP and Al-ACP were significantly lower than the d_m s of all other ACPs subjected to surface modification and marginally lower than the d_m s of ground- (g-ACP) or milled- (m-ACP) solids. By comparing the PSD histograms and the corresponding SEM images (not shown here), it is concluded that the degree of particle agglomeration in Zn-ACP and Al-ACP has been modestly reduced—the quantification of the effect was not attempted. A similar conclusion was made after examining the PSDs and SEMs of g- and m-ACP vs. the control.

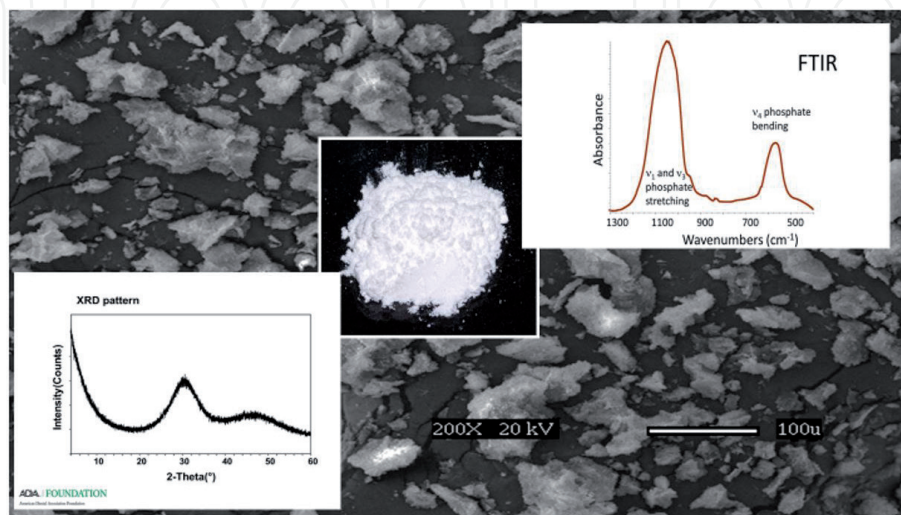


Figure 1. Representative XRD pattern (lower left corner) and FTIR spectrum (upper right corner) of ACP powder (center) with the corresponding SEM image (background).

Additives	Expected interactions/effect(s)
Cations	
Ag ⁺ , Fe ²⁺ , Zn ²⁺ , Al ³⁺ , Fe ³⁺ , Si ⁴⁺ , Zr ⁴⁺	ACP/cation interactions controlled by the cation's ionic potential
Surfactants*	
Anionic-Zonyl FSP	As dispersants, surfactants prevent agglomeration of ACP particles and their coalescence with water
Nonionic-Triton100, Tween 80, Zonyl FSN	
Polymer*	
PEO (M _w 8 K, 100 K, 1000 K)	Polymer stabilizes ACP particles via multiple chelation
Treatments	
Silanization*	
(APTMS, MPTMS)	Silane agents stimulate formation of durable bonds at ACP/resin interface
Grinding	Particle size reduced by friction
Ball milling	Particle size reduced and PSD homogenized via high-energy impact and collision

*Acronyms are defined in the appended list of abbreviations.

Table 1.
Surface modification of ACP: ab initio additives and secondary treatments.

The significant increase in d_m of polymer-ACPs, on the other hand, could be attributed to the effect similar to “polymer bridging” seen in apatite/high-molecular-weight (Mw) polyacrylate system [18]. In theory, poly(ethylene oxide) (PEO)/ACP interactions are controlled by the conformational changes in the adsorbed polymer, collision rate between the particles, and/or aggregate breakup due to fluid shear [20]. However, the exact controlling mechanism is yet to be determined.

The total content of surface-bound and/or structural water in all ACPs was unaffected by the treatment (on average 16.0 ± 1.2 mass%) and compared well with the control (15.8 ± 3.9 mass%). Ideally, the lower intrinsic water content associated with less agglomerated ACP filler is desired to ensure favorable WS and ion release. WS of dental composites is generally controlled by structure/composition of the resin matrix. In case of ACP composites, the hydrophilic filler increases the amount of water absorbed. In ACP/Bis-GMA composites [21], filler/resin interface is inundated by the numerous voids that may enhance water diffusion and hydration of the filler. These processes are better controlled in m-ACP composites [14].

A simple BFS [22] screening of Bis-GMA-based ACP composites (**Figure 2**) revealed the following order of mechanical stability upon extended (up to 3 months) exposure to aqueous environment: (m-ACP \geq g-ACP \geq Zn-ACP = Zr-ACP = silanized ACP) \geq control (unmodified) ACP \geq (Si-ACP \geq surfactant-ACPs) \geq (Al-ACP = PEO-ACP). The observed decrease in BFS of ACP composites can, generally, be attributed to either reduction in ACP’s intactness caused by spatial changes that occur in parallel to ion release, the internal ACP to apatite conversion, or increased WS. The experimental finding that, after aqueous immersion, the BFS of Al-ACP and PEO-ACP composites deteriorated independently of their PSDs (d_m of PEO-ACP was more than six times larger than that of Al-ACP, while their BFS was practically identical) suggests that fillers PSD has only a minor, if any, role in composite’s ability to resist plasticization/degradation upon water exposure.

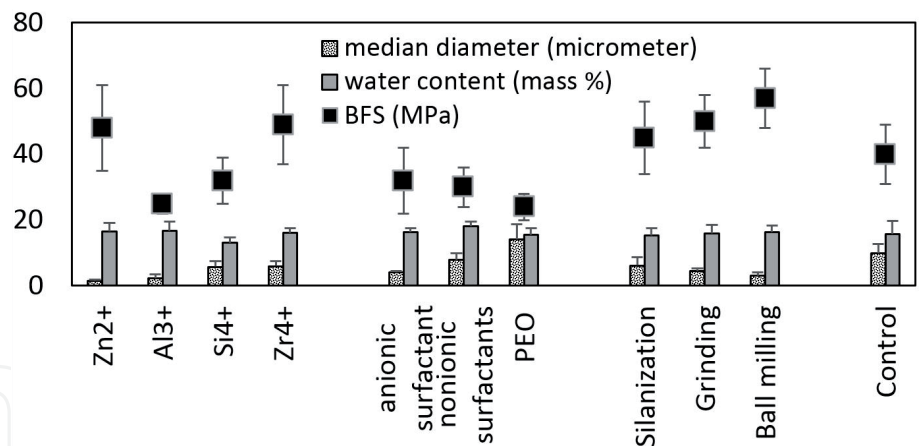


Figure 2. Effect of additives/treatments on PSD and water content of ACP solids and the biaxial flexure strength (BFS) following the aqueous immersion of composite specimens formulated with these fillers and bis-GMA resin. Indicated are mean values of minimum three independent runs and standard deviations (SD, represented by bars). Control ACP: as-ACP made without additives or a secondary treatment.

Our findings contradict an earlier report [23] that PEO strengthened the interface with ACP interface. Better understanding of the observed behavior may require further in-depth mechanical testing and water sorption/desorption evaluations. It appears prudent to consider approaches apart from the undertaken filler treatments, such as choice of monomers utilized in resin formulations, to design composites with optimized performance.

2.2 Resin matrix: fine-tuning a means of improving copolymer properties

The experimental resins were formulated from the commercially available base, diluent, and adhesive monomers activated for light-, chemical-, and/or dual (light and chemical)-cure (LC, CC, and DC, respectively). Monomers utilized in resin formulations and the ranges of their concentrations are listed in **Table 2** (indicated acronyms will be used throughout this chapter). All commercial monomers were utilized as received, without any additional purification.

In LC formulations, all components were blended together and stirred at room temperature until reaching a uniform consistency. In CC formulations, monomers were first combined, their mixture homogenized and then divided into two equal parts by mass. The components of the CC initiating system are added separately to each monomer mixture and stirred magnetically until blended fully. In DC systems, LC and CC step were combined. LC and DC preparations required the use of yellow light to prevent the premature photopolymerization.

Copolymer specimens were prepared by packing resins into Teflon molds, covering each side of the mold with Mylar film and a glass slide, clamping assembly together, and, for LC and DC specimens, curing each side of the assembly with visible light for 2 minutes. Physicochemical tests routinely performed with copolymers involved assessment of degree of vinyl conversion (DVC; near-IR spectroscopy), WS (gravimetric measurements), and BFS.

Methacrylate-based dental resins typically entail high-viscosity base monomer (due to its larger molecular volume decreases polymerization shrinkage (PS) and enhances modulus of cured copolymer) and low-viscosity diluent monomer (due to its smaller molecular volume and greater flexibility enhances DVC and handling properties). Majority of contemporary dental resins is Bis-GMA-/TEGDMA-based. Known drawbacks of Bis-GMA-based systems are relatively low DVCs, high PS, and susceptibility to hydrolytic and enzymatic degradation upon

Component	Chemical name	Acronym	Content (mass %)
Base monomers	2,2-Bis[p-(2'-hydroxy-3'-methacryloxypropoxy) phenyl] propane	Bis-GMA	≥68.4
	Ethoxylated bisphenol A dimethacrylate	EBPADMA	≤68.4
	Urethane dimethacrylate	UDMA	≤92.4
Diluent monomers	Ethyl-α-hydroxymethyl acrylate	EHMA	≤29.2
	2-hydroxyethyl methacrylate	HEMA	≤30.4
	Poly(ethylene glycol)-extended UDMA	PEG-U	≤29.1
	Triethylene glycol dimethacrylate	TEGDMA	≤50.2
Adhesive monomers	Methacryloyloxyethyl phthalate	MEP	≤5.0
Initiators	<i>Light cure</i>		
	Camphorquinone	CQ	0.2
	Ethyl-4 N,N-dimethylamino benzoate	4EDMAB	0.8
	<i>Chemical cure</i>		
	Benzoyl peroxide	BPO	2
	2,2-Dihydroxyethyl-p-toluidine	DHEPT	1

Table 2.
Methacrylate monomers and the components of polymerization-initiating systems utilized to fabricate the experimental resins.

exposure to oral fluids. In our resin fine-tuning studies, we have been exploring the utility of EBPADMA and UDMA as the alternative base monomers and EHMA, HEMA, and PEG-U as the alternative diluent monomers. These studies are expected to yield valuable information on the interplay between the resin’s hydrophilicity/hydrophobicity, DVC, and mechanical stability and their effects on thermodynamic stability and mechanical performance of ACP composites fabricated with these resins.

Results of DVC and BFS screenings of Bis-GMA-, EBPADMA-, and UDMA-based resins are compiled in **Figure 3**. The DVC values attained in our experimental formulations (ranging from 81.4 to 88.2%) with varying diluent and/or adhesive monomers (**Table 2**) significantly exceeded the typical DVC values reported for Bis-GMA/TEGDMA copolymers (60–70% [24]).

DVCs attained in Bis-GMA ($81.4 \pm 2.5\%$), EBPADMA ($84.8 \pm 5.5\%$), and UDMA ($88.2 \pm 2.2\%$) copolymers were significantly different ($P < 0.05$; Tukey post hoc test) only for UDMA vs. Bis-GMA systems. The BFS values, apparently increasing in going from Bis-GMA to EBPADMA to UDMA copolymers ($R^2 = 0.9685$), were significantly different ($P < 0.05$) only between UDMA and Bis-GMA copolymers. WS (data not shown) was not significantly affected by the resin’s compositional changes. In all three groups, maximum WS (values ranged from 2.3 to 3.0 mass%) was achieved within 2 weeks of aqueous immersion. Slight differences between the measured WS values could be related primarily to the inclusion of more hydrophilic (HEMA, TEGDMA) or less hydrophilic (EHMA, PEG-U) monomers in the resin matrix. It is, however, highly significant that all systems maintained the WS profiles that support a sustained ion release from the composites (see Section 2.3).

2.3 ACP composites: fabrication, physicochemical, mechanical, and biological assessments

To fabricate composites, resin (60 mass%) and ACP filler (40 mass%) were combined by hand spatulation. The homogenized paste was kept overnight under vacuum to eliminate the entrapped air before being utilized for preparation of testing specimens by employing the procedures identical to those for the preparation of copolymer specimens. Besides DVC, BFS, WS, and PS testing, physicochemical and biological evaluation of composites also entailed polymerization shrinkage stress (PSS), shear bond strength (SBS) to dentin, ion release kinetics, leachability of unreacted species, remineralization efficacy, and in vitro cytotoxicity tests.

DVCs (**Figure 4**) of Zr-ACP composites formulated with various resins significantly (ANOVA, Tukey test; $P < 0.05$) increased in going from Bis-GMA to EBPADMA to UDMA matrix. Higher DVC in UDMA systems could possibly be explained by the higher reactivity of UDMA than Bis-GMA and/or EBPADMA [25]. Resin composition, however, had no effect on the BFS of composites being ~50% lower than the BFS of their copolymer counterparts (compare BFS data in **Figure 4** vs. **Figure 3**). The reduction in BFS in UDMA-based composites (1.7%) was significantly lower ($P < 0.05$) than reduction in BFS in Bis-GMA- to EBPADMA-based composites (10.0 and 4.4%, respectively). This finding suggests that random

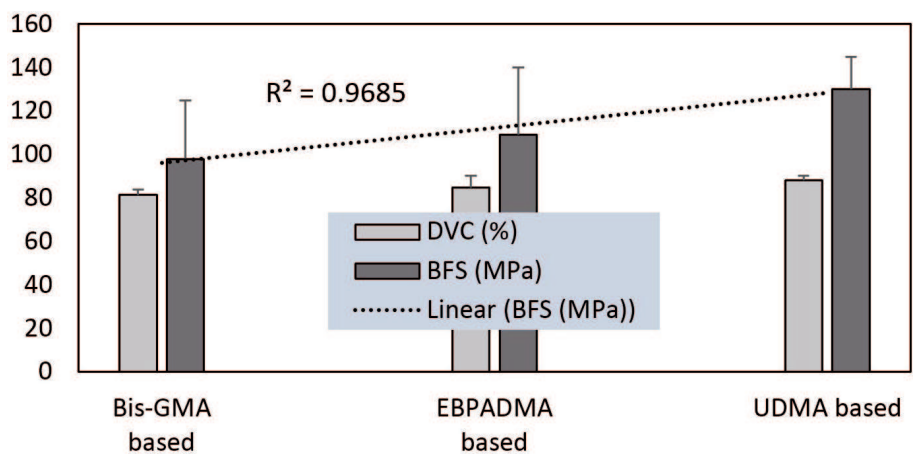


Figure 3. DVC and BFS of LC binary, ternary, and quaternary bis-GMA-, EBPADMA-, and UDMA-based copolymers. Indicated are mean values + SD (represented by bars) for $n \geq 24$ (DVC) and $n \geq 12$ (BFS).

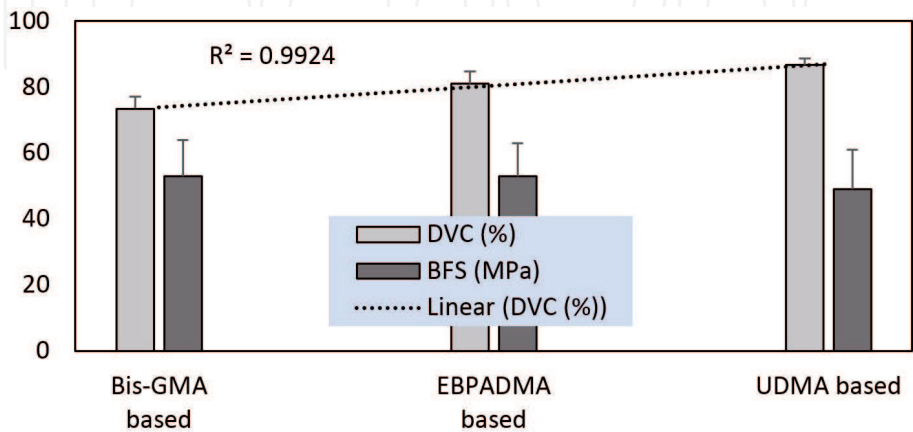


Figure 4. DVC and BFS of LC Zr-ACP bis-GMA-, EBPADMA-, and UDMA-based composites. Indicated are mean values + SD (represented by bars) for $n \geq 24$ (DVC) and $n \geq 12$ (BFS).

distribution of Zr-ACP agglomerates [21], rather than the resin matrix composition, controls the mechanical performance of composites.

Generally, WS {(3.3–3.8) mass%}, SBS {(15.3–17.5) MPa}, and PS {(6.5–7.0) vol%} results revealed no distinguishable differences between the Bis-GMA-, EBPADMA-, and UDMA-based composites. The observed increase in WS of composites vs. their copolymer counterparts (27–43%) was due to ACP's affinity to the environmental water. It is significant that, in terms of SBS, ACP composites performed as well as Sr-glass filled composites [17], thus providing the remineralizing component to the primary restorative function without impediment of short- and midterm dentin bonding. High PS (undesirable) seen in all three experimental groups go hand in hand with the high DVCs (desirable) attained in these systems. These high PS values are likely due to the increased hydrogen bonding occurring in all experimental matrices leading to the densification of polymerization [26]. It is particularly important that, in UDMA-based composites, high PS can be offset by a significant hygroscopic expansion (HE; up to 13.6 vol%; data not shown). The compensating effect of HE on PS has been demonstrated in [27–29]. We were unable to establish any correlation between the PS and PSS in our experimental systems. Although contributions on this subject in dental literature are considerable [30–33], there is a question whether processing factors such as configuration factor (C-factor) besides the filler type and its load level, resin composition, and polymerization mode control the composite performance [34].

Comparative kinetic study of ion release from Bis-GMA- and EBPADMA-based composites showed a systematic increase in solution Ca and PO_4 concentrations with the increased filler level in the composite and with time of aqueous immersion. Values of the ion activity product (IAP) used to calculate the relative supersaturation of the solutions with respect to the stoichiometric hydroxyapatite (details on these calculations are provided in [35]) are presented in **Figure 5**. The ion release kinetics was practically identical in both types of composites. It was shown that a minimum of 35 mass% of ACP filler in composite is needed to create a sustained solution supersaturation inductive to apatite formation. The overall ion release kinetics in these systems was most likely controlled by the level of hydrophilic HEMA monomer in the resin phase. By more easily absorbing the water needed for ion diffusion, HEMA regulated the internal mineral saturation levels.

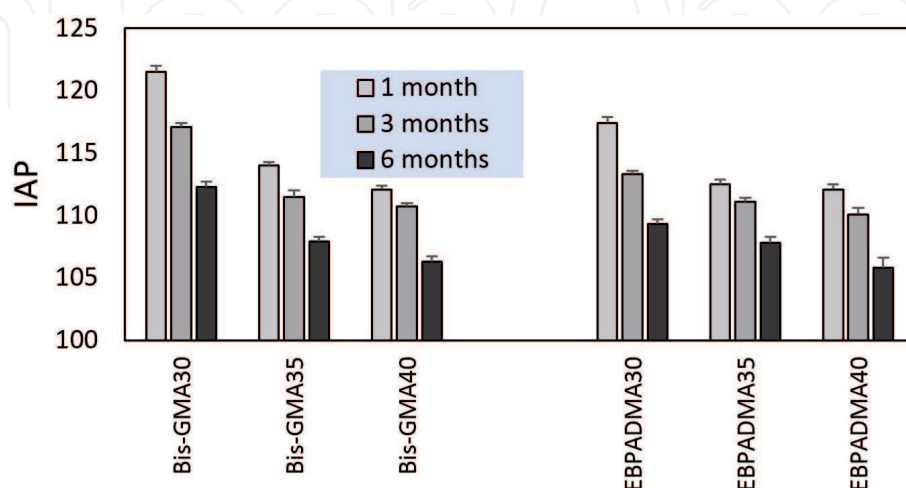


Figure 5. Mean value + SD (indicated by bars) of the ion activity product (IAP) of the solutions containing Ca and PO_4 ions released from bis-GMA- and EBPADMA-based composites with various ACP levels (30, 35, or 40 mass%) at different times of immersion (1, 3, or 6 months) in saline solutions (23°C; continuous magnetic stirring). Number of repetitive experiments $n = 3/\text{group}$.

In our studies, we conveniently use the DVC as a predictor of leachability (the higher the DVC, the lower the likelihood of unreacted monomers to leach) from the restorations. To quantify leaching from the UDMA/PEG-U/HEMA/MEP (UPHM) copolymers and their ACP composites, we have employed ^1H -NMR spectroscopy. The accelerated leaching was mimicked by using acetone as extraction medium. Results are presented in **Figure 6**. Leaching (expressed as a mass fraction of the initial amount incorporated in the resin and normalized to the equivalent amount of the resin for composite specimens) decreased in the following order: 4EDMA B > MEP > UDMA > PEG-U > HEMA > CQ (undetectable). Introducing ACP filler into UPHM matrix did not have an impact on the leachability profile. In highly cross-linked UPHM matrix, polymer chain mobility remained small in both copolymers and composites, thus limiting the pathways for unreacted monomers to leach out from the specimens. The disproportionate leachability of 4EDMAB, a component of the LC initiator system, is most likely due to its excess relative to CQ (CQ:4EDMAB mass ratio 1:4), which appears to be fully consumed during polymerization and is undetectable in the extracts. Since HEMA is known for its increased toxicity and adverse side effects due to metabolizing to methacrylic acid [36], it is of high significance that the level of leachable HEMA from UPHM copolymers and composites is drastically (several orders of magnitude) lower than typically seen in HEMA-containing resins and composites. In addition, levels of leachable UDMA from UPHM matrices are more than twice lower than the amounts of leached UDMA from the experimental UDMA/TEGDMA formulations [37]. In the complex, high-DVC UPHM network, the mobility of the unreacted low-molecular-weight HEMA is limited or reduced, and its elution to the environment is prevented.

In vitro cytotoxicity screening should be performed in conjunction with the leachability tests to better predict the material's impact at cellular level. To mimic early ACP composite/cell interactions, we have performed the extraction experiments and assessed cell morphology and cell viability according to the recommended standards [38–40]. The osteoblast-like MC3T3-E1 cells were seeded on ethanol-sterilized material disks, incubated in the extracts for 24 h, then evaluated in situ by optical microscopy, and assessed for cytotoxicity by tetrazolium-based {3-(4,5-dimethylthiazol-2-yl)-2,5-diphenyltetrazolium bromide; MTT} assay. Detailed protocols are described in [41]. The results of the cytotoxicity evaluation of UPHM composites are presented in **Figure 7**. Cell morphology (**Figure 7**, inlets) changed from polygonal, spread (cells exposed to pure medium and extracts from UPHM copolymer and compressed ACP filler) to spherical (cells incubated in

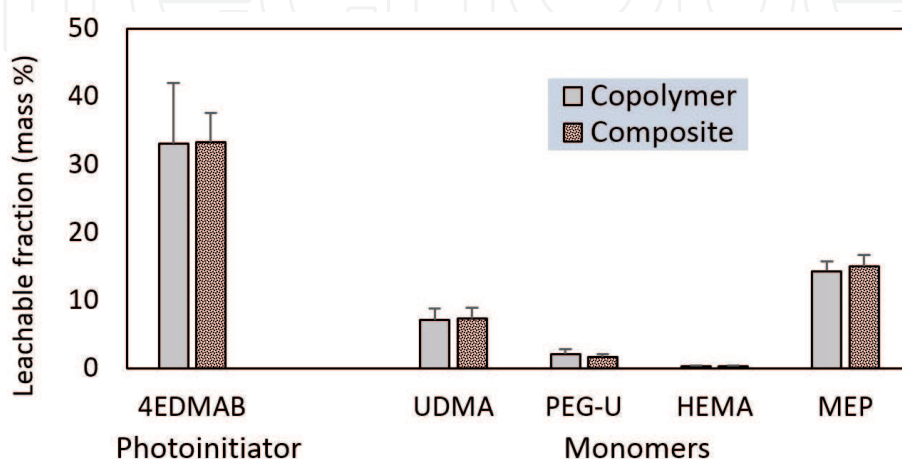


Figure 6. Leachables (mean value + SD (represented by bars); $n = 3/\text{group}$) detected by ^1H -NMR spectroscopic method in acetone extracts from LC UPHM copolymers and their ACP composites (in composite series; values are normalized with respect to the initial resin amount).

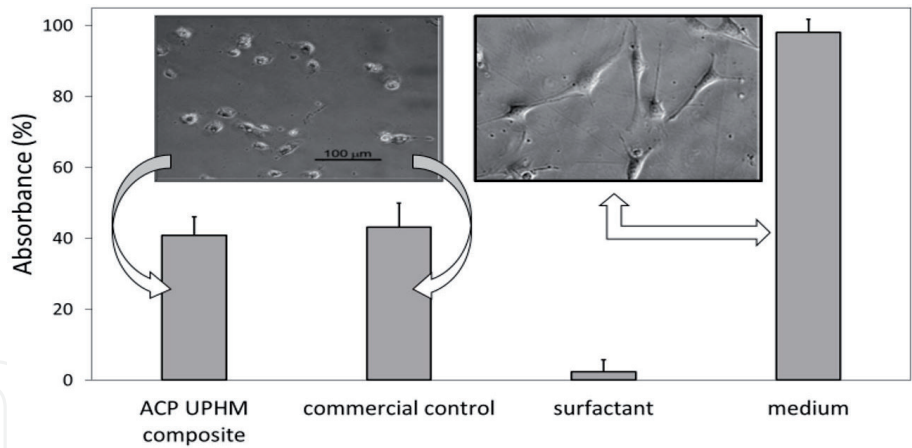


Figure 7. Viability of osteoblast-like cells upon exposure to the extracts from ACP UPHM composite, commercial composite, medium + surfactant, and medium only. Shown are mean values \pm SD (indicated by bars) for three repetitive runs in each group. Optical micrographs indicating typical changes in cell morphology upon exposure to the extracts from composites (left side) and pure medium (right side).

extracts from the experimental ACP UPHM composite and commercial control). Viability of contracted cells (i.e., those exposed to extracts from both composites) was reduced approximately twofold compared to the polygonal cell incubated in medium only. Similar morphological changes and slow cell proliferation observed in bone-regenerating hydrogels [42] are reportedly linked to the alterations in cell nucleus and mineralization of osteoprogenitors [43]. While fuller understanding of the cellular effects is certainly needed, it is encouraging that reduction in cell viability seen with our experimental composites was comparable with the commercial control.

Remineralization efficacy studies were undertaken to demonstrate the ability of ACP composites to regenerate demineralized tooth structures. Details on the microradiographic in vitro evaluations of the changes in mineral content of the demineralized bovine and/or human enamel subjected to aggressive acid attacks, representative prolonged exposure in oral milieu, are provided in [44, 45], respectively. These studies indicate that lost tooth mineral is indeed regenerated upon application of ACP composites (**Figure 8**). Mineral recovery with ACP Bis-GMA-based composites significantly exceeded the remineralization effect of

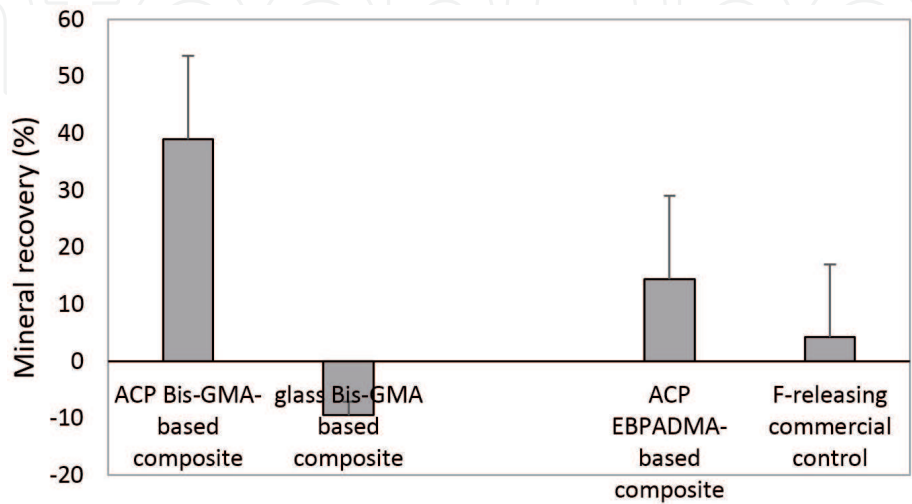


Figure 8. Mineral recovery (or loss) following the pH regimens representing pH cycling in oral environment. Shown are mean values \pm SD (indicated by bars) obtained from a minimum of eight micrographic images/experimental group.

the glass-filled control. On average, more than threefold increase of mineral content attained with ACP EBPADMA-based composites compared to F-releasing control was, however, statistically insignificant due to a large data scattering. It is particularly important that the regenerative action took place throughout the lesions in contrast to F-supported repair which is typically limited to a subsurface region.

2.4 Adding antimicrobial functionality to dental restoratives

To prolong service life, the next generation of polymeric dental restoratives is envisioned to possess bioactive properties. Today, developments of dental materials with embedded AM properties are relatively frequently reported. One of the first quaternary ammonium (QA) methacrylates integrated into Bis-GMA/TEGDMA matrix has been reported 20 years ago [46]. More recently, two polymerizable ionic dimethacrylates (2-(methacryloyloxy)-N-(2-(methacryloyloxy)ethyl)-N,N-dimethylethan-1-aminium bromide (IDMA1) and N,N'-([1,1'-biphenyl]-2,2'-diylbis(methylene))bis(2-(methacryloyloxy)-N,N-dimethylethan-1-aminium) bromide (IDMA2)) were proposed for use in dental applications [47, 48]. Purity of the synthesized materials was not reported, and the structural characterizations appeared incomplete. The IDMA s have been validated by nuclear magnetic resonance, mass spectroscopy, and FTIR spectroscopies [49, 50]. These studies also included direct contact cytotoxicity testing at biologically relevant concentrations. To date, AM assessments of the fully characterized IDMA s are remaining.

For the advancement of Class V restoratives, our goal was to evaluate the AM properties of purified/validated IDMA1 and IDMA2 integrated in dental copolymers, using *Streptococcus mutans* (planktonic and biofilm).

IDMA copolymer disks (6 mm diameter) were fabricated by adding IDMA1 or IDMA2 (10 wt %) to light-activated UDMA/PEG-U/EHMA (hereafter UPE) resin. For both planktonic and biofilm testing, UPE disks were used as a negative control group. After fabrication, all copolymer disks were subjected to aqueous extraction (72 h, 37°C). After drying, specimens were sterilized using an Anprolene gas sterilization chamber (Andersen Products, Inc., Haw River, NC). Prior to bacterial testing, specimens were degassed for ≥ 5 days.

A bioluminescent *S. mutans* strain JM10 [51] (derivative of wild-type UA159) was used to assess the antibacterial properties, the IDMA s, employing a real-time bioluminescent assay developed by Florez et al. [52]. In UPE resin matrix, 10% IDMA1 reduced ($P \leq 0.005$) the colonization of *S. mutans* biofilms threefold (**Figure 9**). The initial report describing the synthesis of IDMA1 and incorporation into Bis-GMA-TEGDMA resin conducted *S. mutans* testing with phosphate-buffered saline (i.e., no extrinsic proteins) [48]. Therein, they report reduced bacterial colonization for IDMA1 concentrations of 10, 20, or 30%. In the presence [53, 54] or absence [55] of ACP, others have demonstrated that IDMA1 fabricated with Bis-GMA/TEGDMA results in a modest (1.4–1.7-fold decrease in metabolic activity of biofilm) AM function in a protein-rich environment. To enhance AM activity, IDMA1 in combination with silver nanoparticles and/or nano-ACP was integrated into dental materials [53–56].

AM activity of IDMA2 has not been previously reported. Compared to the UPE control resin, our experiments demonstrated that IDMA2-UPE copolymer reduced ($P \leq 0.005$) the colonization of *S. mutans* biofilms 1.6-fold (**Figure 9**). However, the AM activity of IDMA2 was less ($P \leq 0.05$) than that observed with IDMA1. This difference may be due to steric hindrance resulting from the presence of aromatic rings in IDMA2. Further, it is noteworthy that IDMA2 can exist as a mixture of conformers. Thus, it is conceivable that the conformer (with decreased steric

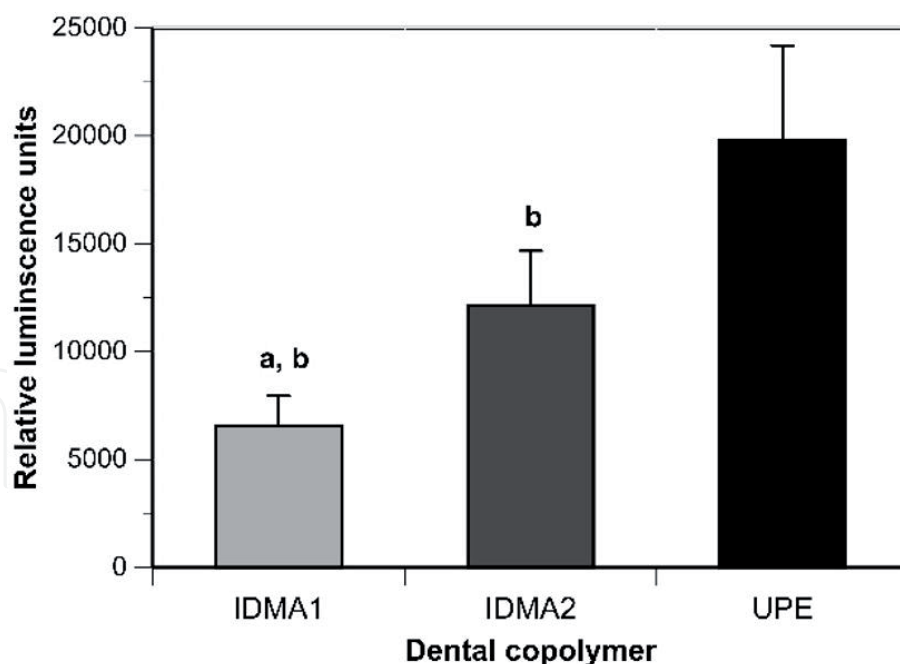


Figure 9.

Streptococcus mutans biofilm growth by the experimental IDMA-UPE (10 wt %) copolymers compared to UPE resin. Presented are mean values \pm SD (indicated by bars) of 5 specimens/experimental group. ^a $P \leq 0.05$ compared to IDMA2; ^b $P \leq 0.005$ compared to UPE resin.

hindrance) could exhibit greater AM activity. Future research that enables preparations, enriched for each conformer, is warranted to determine whether AM activity of IDMA2 can be enhanced.

For planktonic bacterial testing, *S. mutans* UA-159 (ATCC® 700610) cultures were established in Todd Hewitt broth (THB). Copolymer disks were seeded with *S. mutans* suspension ($\sim 3 \times 10^7$ colony-forming units/disk). To maximize the contact between the copolymer and bacteria, a second disk was placed atop. This assembly was incubated 2 h at 37°C in a 5% CO₂ environment. The samples were then placed in 1 ml of THB and utilized to prepare 10-fold serial dilutions. Of the resulting suspensions, 100 μ l were distributed onto the surface of THB agar plates. Colony-forming units were the unit of measure used to approximate the number of viable *S. mutans* cells after exposure to the IDMA-UPE copolymers. Among the IDMA groups, the number of colony-forming units observed was not statistically different from one another or the UPE control resin (data not shown).

Altogether, the full AM potential of the IDMA has not yet been realized. For example, the current IDMA restorative material formulations are likely to have charges randomly distributed throughout the material. It is conceivable that chemical engineering advances (i.e., material gradient or layers) could favor the orientation of the N⁺ charges while maintaining the material mechanical properties. Secondly, previous reports demonstrated that the presence of proteins dampens the AM capability of QA methacrylates (reviewed by [57]). To overcome this problem, a commercially available protein repellent, 2-methacryloyloxyethyl phosphorylcholine (MEPC), has been integrated into AM dental material [58]. However, because of possible binding of the remineralizing calcium ions by MEPC [59], MEPC may have a deleterious effect on the remineralization capacity of the restorative material. Generally, to date, there is a paucity of information regarding the nature of proteins binding to the surface of QA methacrylates. Elucidation of the protein-material interactions would yield valuable information to develop a strategy to maximize AM efficacy of materials with a charge-based AM mechanism of action. Further, these data could facilitate the advancement of materials, modified to target specific proteins (i.e., via molecular imprinting).

3. Conclusions

Bioactive, ACP-based polymeric dental composites ACP have tremendous appeal due to their intrinsic ability to regenerate lost tooth mineral. ACP composites release remineralizing Ca and PO₄ ions in a sustained fashion, thus providing a long-term protection against acid challenges in the oral environment. However, with respect to the mechanical strength and toughness, ACP-based composites are inferior to silanized glass-filled counterparts and can only be used in nonstress-bearing applications. The uncontrolled ACP particle agglomeration typically leads to the poor ACP filler/resin interactions that destabilize filler/polymer interface. A desired, more homogeneous PSD of ACP filler is achievable via mechanical treatments, preferably high-energy milling. Surface modifications of ACP were proven less effective in that respect. With HEMA as diluent monomer, LC Bis-GMA-, EBPADMA-, and UDMA-based copolymers and their ACP composites typically attain high-DVC values that would suggest a minimal leaching of unreacted monomeric species from these materials. Expectedly, these high DVCs are accompanied with high PS. In UDMA-based systems, high PS is likely to be offset by a significant HE. High remineralization capabilities are achieved with EBPADMA or UDMA as base monomers and HEMA or EHMA plus PEG-U as diluent monomers. The most recent efforts in our group focus on design of bifunctional, remineralizing, and AM ACP composites that may find utility as new Class V restoratives. These materials are currently being assessed for their in vitro cytotoxicity and AM properties. The evaluations coupled with the leachability studies need to be completed before embarking on animal testing and/or human clinical trials involving AM ACP dental composites.

Acknowledgements

The work presented in this chapter was supported by the National Institute of Dental and Craniofacial Research (grants DE 13169 and DE 26122), American Dental Association (ADA), and ADA Foundation. Special thanks to collaborators (Sharukh S. Khajotia, Fernando L. Esteban Florez, and Rochelle D. Hiers) at the University of Oklahoma Health Sciences Center, College of Dentistry, for conducting biofilm testing. Donation of the monomers by Esstech, Essington, PA, is gratefully acknowledged.

Conflict of interest

Authors declare no conflict of interest.

A. Appendix: list of abbreviations

ACP	amorphous calcium phosphate
ADA	American Dental Association
ADAF	American Dental Association Foundation
Al-ACP	aluminum-modified ACP
AM	antimicrobial
APTMS	3-aminopropyltrimethoxysilane
as-ACP	as synthesized ACP
BFS	biaxial flexure strength

Bis-GMA	2,2-bis[p-(2'-hydroxy-3'-methacryloxypropoxy) phenyl] propane
BPO	benzoyl peroxide
CaP	calcium phosphate
CC	chemical-cure
CQ	camphorquinone
DC	dual-cure
DHEPT	2,2-dihydroxyethyl-p-toluidine
d _m	median diameter
DVC	degree of vinyl conversion
EBPADMA	ethoxylated bisphenol A dimethacrylate
4EDMAB	ethyl-4 N,N-dimethylamino benzoate
EHMA	ethyl- α -hydroxymethyl acrylate
FTIR	Fourier-transform infrared
g-ACP	ground ACP
HE	hygroscopic expansion
HEMA	2-hydroxyethyl methacrylate
IAP	ion activity product
IDMA	ionic dimethacrylate
IDMA1	2-(methacryloyloxy)-N-(2-(methacryloyloxy)ethyl)-N,N-dimethylethan-1-aminium bromide
IDMA2	N,N'-([1,1'-biphenyl]-2,2'-diylbis(methylene))bis(2-(methacryloyloxy)-N,N-dimethylethan-1-aminium) bromide
LC	light-cure
m-ACP	milled ACP
MEP	methacryloyloxyethyl phthalate
MEPC	2-methacryloyloxyethyl phosphorylcholine
MPTMS	methacryloxypropyltrimethoxy silane
MTT	3-(4,5-dimethylthiazol-2-yl)-2,5-diphenyltetrazolium bromide assay
Mw	molecular weight
n	number of specimens/experimental runs
PEG	poly(ethylene glycol)
PEG-U	PEG-extended UDMA
PEO	poly(ethylene oxide)
PS	polymerization shrinkage
PSD	particle size distribution
PSS	polymerization shrinkage stress
QA	quaternary ammonium
SBS	shear bond strength
SEM	scanning electron microscopy
SD	standard deviation
Si-ACP	silica-modified ACP
TEGDMA	triethylene glycol dimethacrylate
TGA	thermogravimetric analysis
THB	Todd Hewitt broth
Triton 100	C ₁₄ H ₂₂ O(C ₂ H ₄ O) ₁₀ H; nonionic surfactant
Tween 80	C ₂₄ H ₄₃ O ₆ (C ₂ H ₄ O) ₂₀ H; nonionic surfactant
UDMA	urethane dimethacrylate
UPE	UDMA/PEG-U/EHMA resin
UPHM	UDMA/PEG-U/HEMA/MEP resin
XRD	X-ray diffraction
WS	water sorption
Zn-ACP	zinc-modified ACP

Zr-ACP	zirconia-modified ACP
Zonyl FSN	$F(C_2F_4)_x(C_2H_4O)_{1+y}H$; nonionic surfactant ($x = 1-9$; $y = 0-25$)
Zonyl FSP	$F(C_2F_4)_x(C_2H_4O)_yHP(O)(ONH_4)_z$; anionic surfactant ($x = 1-7$; $(y + z) = 3$)

IntechOpen

IntechOpen

Author details

Diane R. Bienek, Anthony A. Giuseppetti and Drago Skrtic*
Research Division, American Dental Association Foundation, Frederick, MD, USA

*Address all correspondence to: drago.skrtic@nist.gov

IntechOpen

© 2019 The Author(s). Licensee IntechOpen. This chapter is distributed under the terms of the Creative Commons Attribution License (<http://creativecommons.org/licenses/by/3.0>), which permits unrestricted use, distribution, and reproduction in any medium, provided the original work is properly cited. 

References

- [1] Dorozhkin SV. Calcium orthophosphates (CaPO_4): Occurrence and properties. *Progress in Biomaterials*. 2016;**5**:9-70. DOI: 10.1007/s40204-015-0045-z
- [2] Eliaz N, Metoki N. Calcium phosphate bioceramics: A review of their history, structure, properties, coating technologies and biomedical applications. *Materials*. 2017;**10**:334. DOI: 10.3390/ma10040334
- [3] Dorozhkin SV. Calcium orthophosphates (Ca_3PO_4) and dentistry. *Bioceramics Development and Applications*. 2016;**6**(2). DOI: 10.4172/2090-5025:1000096
- [4] Bienek DR, Skrtic D. Utility of amorphous calcium phosphate-based scaffolds in dental/biomedical research. *Biointerface Research in Applied Chemistry*. 2017;**7**(1):1989-1994
- [5] Dorozhkin SV. Amorphous calcium orthophosphates: Nature, chemistry and biomedical applications. *International Journal of Materials and Chemistry*. 2012;**2**(1):19-46. DOI: 10.5923/j.ijmc20120201.04
- [6] Glimcher MJ, Bonar LC, Grynpas MD, Landis WJ, Roufosse AH. Recent studies of bone mineral: Is the amorphous calcium phosphate theory valid? *Journal of Crystal Growth*. 1981;**53**:100-119. DOI: 10.1016/9922-0248(81)90058-0
- [7] Grynpas MD, Bonar LC, Glimcher MJ. Failure to detect an amorphous calcium phosphate solid phase in bone mineral: A radial distribution function study. *Calcified Tissue International*. 1984;**36**:291-301. DOI: 10.1007/BF0240533
- [8] Weiner S, Sagi I, Addadi L. Choosing the crystallization path less travelled. *Science*. 2005;**309**:1027-1028. DOI: 10.1126/science.1114920
- [9] Weiner S. Transient precursor strategy in mineral formation of bone. *Bone*. 2006;**39**:431-433. DOI: 10.1016/j.bone2006.02.058
- [10] Mahamid J, Sharir A, Addadi L, Weiner S. Amorphous calcium phosphate is a major component in forming fin bones of zebrafish: Indications for an amorphous precursor phase. *Proceedings of the National Academy of Sciences of the United States of America*. 2008;**105**:12748-12753. DOI: 10.1073/pnas.0806869105
- [11] Beniash A, Metzler RA, Lam RSK, Gilbert PUPA. Transient amorphous calcium phosphate in forming enamel. *Journal of Structural Biology*. 2009;**166**:133-143. DOI: 10.1016/j.jsb2009.02.001
- [12] Eanes ED. Amorphous calcium phosphate. In: Chow LC, Eanes ED, editors. *Monographs in Oral Science*. Vol. 18. Basel: Karger; 2001. pp. 130-147. ISBN: 9783318007046 3318007048
- [13] Heughebaert JC, Montel G. Conversion of amorphous calcium phosphate into apatitic tricalcium phosphate. *Calcified Tissue International*. 1982;**34**:S103-S108. DOI: 10.1007/BF02426637
- [14] O'Donnell JNR, Antonucci JM, Skrtic D. Illuminating the role of agglomerates on critical physicochemical properties of amorphous calcium phosphate composites. *Journal of Composite Materials*. 2008;**42**:2231-2246. DOI: 10.1177/0021998308094797
- [15] Eanes ED, Gillesen IH, Posner AS. Intermediate states in the precipitation of hydroxyapatite. *Nature*.

1965;**208**(5008):365-367. DOI:
 10.1038/208365a0

[16] Antonucci JM, Skrtic D. Bioactive and biocompatible polymeric composites based on amorphous calcium phosphate. In: Ramalingam M, Tiwari A, Ramakrishna S, Kobayashi H, editors. *Integrated Biomaterials for Medical Applications*. Salem: Scrivener Publishing; 2012. pp. 67-119. DOI: 10.1002/9781118482513.ch3

[17] O'Donnell JNR, Skrtic D. Degree of vinyl conversion, polymerization shrinkage and stress development in experimental endodontic composite. *Journal of Biomimetics Biomaterials and Tissue Engineering*. 2009;**4**:1-12. DOI: 10.4028/www.scientific.net/JBBTE.4.1

[18] Skrtic D, Antonucci JM. Dental composites: Bioactive polymeric amorphous calcium phosphate-based. In: *Encyclopedia of Biomedical Polymers and Polymeric Biomaterials*. New York: Taylor and Francis; 2015. pp. 2443-2262. DOI: 10.1081/E-EBPP-120051063

[19] Ofir PBY, Govrin-Lipman R, Garti N, Furedi-Milhofer H. The influence of polyelectrolytes on the formation and transformation of amorphous calcium phosphate. *Crystal Growth & Design*. 2004;**4**(1):177-183. DOI: 10.1021/cg034148g

[20] Antonucci JM, Liu DW, Skrtic D. Amorphous calcium phosphate-based composites: Effect of surfactants and poly (ethylene oxide) on filler and composite properties. *Journal of Dispersion Science and Technology*. 2007;**28**(5):819-824. DOI: 10.1080/01932690701346255

[21] Skrtic D, Antonucci JM, Eanes ED, Eidelman N. Dental composites based on hybrid and surface-modified amorphous calcium phosphates. *Biomaterials*. 2004;**25**:1141-1150. DOI: 10.1016/j.biomaterials.2003.08.001

[22] ASTM F394-78 (re-approved 1991). Standard test method for biaxial flexure strength of ceramic substrates

[23] Li Y, Weng W, Cheng K, Du P, Shen G, Wang J, et al. Preparation of amorphous calcium phosphate in the presence of poly (ethylene glycol). *Journal of Materials Science Letters*. 2003;**22**(14):1015-1016. DOI: 10.1023/A:1024741426069

[24] Marovic D, Panduric V, Tarle Z, Ristic M, Sariri K, Demoli N, et al. Degree of conversion and microhardness of dental composite resin materials. *Journal of Molecular Structure*. 2013;**1044**:299-302. DOI: 10.1016/j.molstruc.2012.10.062

[25] Morgan DR, Kalachandra S, Shobha HK, Gunduz N, Stejskal EO. Analysis of a dimethacrylate copolymer (bis-GMA and TEGDMA) network by DSC and ¹³C solution and solid-state NMR spectroscopy. *Biomaterials*. 2000;**21**(18):1897-1903. DOI: 10.1016/S142-9612(00)00067-3

[26] Skrtic D, Antonucci JM. Dental composites based on amorphous calcium phosphate–resin composition/physicochemical properties study. *Journal of Biomaterials Applications*. 2007;**21**(4):375-393. DOI: 10.1177/0885328206064823

[27] Momoi Y, McCabe JF. Hygroscopic expansion of resin based composites during 6 months water storage. *British Dental Journal*. 1994;**176**(3):91-96. DOI: 10.1038/sj.bdj.4808379

[28] Huang C, Tay FR, Cheung GSP, Kei LH, Wei SHY, Pashley DH. Hygroscopic expansion of compomer and a composite on artificial gap reduction. *Journal of Dentistry*. 2002;**30**(1):11-19. DOI: 10.1016/S0300-5712(01)00053-7

[29] Suiter EA, Watson LE, Tantbirojn C, Lou JSB, Versluis A. Effective expansion: Balance between shrinkage

and hygroscopic expansion. *Journal of Dental Research*. 2016;**95**(5):543-549. DOI: 10.1177/0022034516633450

[30] Braga LL, Ferracane JL. Contraction stress related to degree of conversion and reaction kinetics. *Journal of Dental Research*. 2002;**81**(2):114-118. DOI: 10.1177/0810114

[31] Ferracane JL. Developing a more complex understanding of stresses produced in dental composites during polymerization. *Dental Materials*. 2005;**21**(1):36-42. DOI: 10.1016/j.dental.2004.10.004

[32] Kleverlaan CJ, Feizler AJ. Polymerization shrinkage and contraction stress of dental resin composites. *Dental Materials*. 2005;**21**(1):1150-1157. DOI: 10.1016/j.dental.2005.02.004

[33] Choi KK, Condon JR, Ferracane JL. The effects of adhesive thickness on polymerization contraction stress of composite. *Journal of Dental Research*. 2000;**79**(3):812-817. DOI: 10.1177/00220345000790030501

[34] Antonucci JM, Giuseppetti AA, O'Donnell JNR, Schumacher GE, Skrtic D. Polymerization stress development in dental composites: Effect of cavity design factor. *Materials*. 2009;**2**(1):169-180. DOI: 10.3390/ma2010169

[35] O'Donnell JNR, Langhorst SE, Fow MD, Skrtic D. Light-cured dimethacrylate-based resins and their composites; Comparative study of mechanical strength, water sorption and ion release. *Journal of Bioactive and Compatible Polymers*. 2008;**23**:207-226. DOI: 10.1177/0883911508089932

[36] Durner J, Walther UI, Zaspel J, Hickel R, Reich FX. Metabolism of TEGDMA and HEMA in human cells. *Biomaterials*. 2010;**31**:818-823. DOI: 10.1016/j.biomaterials.2009.09.097

[37] Floyd CJE, Dickens SH. Network structure of bis-GMA- and UDMA-based resin systems. *Dental Materials*. 2006;**22**:1143-1149. DOI: 10.1016/j.dental.2005.10.009

[38] International Standard ISO10993-5. Biological evaluation of medical devices- Part 5. Tests for cytotoxicity; In vitro methods. Geneva, Switzerland: International Organization for Standardization; 1992

[39] International Standard ISO7405. Dentistry-preclinical evaluation of biocompatibility of medical devices used in dentistry. Test methods for dental materials. Geneva, Switzerland: International Organization for Standardization; 1997

[40] ANSI/ADA Specification No. 41. Recommended standard practices for biological evaluation of dental materials. 2005

[41] Simon CG, Antonucci JM, Liu DW, Skrtic D. *In vitro* cytotoxicity of amorphous calcium phosphate composites. *Journal of Bioactive and Compatible Polymers*. 2005;**20**(3):279-295. DOI: 10.1177/0883911505061854

[42] Chatterjee K, Lin-Gibson S, Wallace WE, Parekh SH, Lee YJ, Cicerone MT, et al. The effect of 3D hydrogel scaffold modulus on osteoblast differentiation and mineralization revealed by combinatorial screening. *Biomaterials*. 2010;**39**(19):5051-5062. DOI: 10.1016/j.biomaterials.2010.03.024

[43] Dalby MJ, Biggs MJP, Gadegaard N, Kalna G, Wilkinson CDW, Oreffo ROC. The control of human mesenchymal cell differentiation using nanoscale symmetry and disorder. *Nature Materials*. 2007;**6**(12):997-1003. DOI: 10.1038/nmat2013

[44] Skrtic D, Hailer AW, Takagi S, Antonucci JM, Eanes ED. Quantitative assessment of the efficacy of amorphous

calcium phosphate/methacrylate composites in remineralizing caries-like lesions artificially produced in bovine enamel. *Journal of Dental Research*. 1996;**75**(9):1679-1686. DOI: 10.1177/00220345596075091001

[45] Langhorst SE, O'Donnell JNR, Skrtic D. *In vitro* remineralization effectiveness of polymeric ACP composites: Quantitative micro-radiographic study. *Dental Materials*. 2009;**25**:884-891. DOI: 10.1016/j.dental.2009.01.094

[46] Imazato S, Tarumi H, Kato S, Ebisu S. Water sorption and color stability of composites containing the antibacterial monomer MDPB. *Journal of Dentistry*. 1999;**27**(4):279-283

[47] Antonucci JM. Polymerizable biomedical composition. US patent 8217081; July 2012

[48] Antonucci JM, Zeiger DN, Tang K, Lin-Gibson S, Fowler BO, Lin NJ. Synthesis and characterization of dimethacrylates containing quaternary ammonium functionalities for dental applications. *Dental Materials*. 2012;**28**(2):219-228. DOI: 10.1016/j.dental.2011.10.004

[49] Bienek DR, Frukhtbeyn SA, Giuseppetti AA, Okeke UC, Pires RM, Antonucci JM, et al. Ionic dimethacrylates for antimicrobial and remineralizing dental composites. *Annals of Dentistry and Oral Disorders*. 2018;**108**. PMID:30854515

[50] Bienek DR, Frukhtbeyn SA, Giuseppetti AA, Okeke UC, Skrtic D. Antimicrobial monomers for polymeric dental restoratives: Cytotoxicity and physicochemical properties. *Journal of Functional Biomaterials*. 2018;**9**(1):20. DOI: 10.3390/jfb9010020

[51] Merritt J, Kreth J, Qi F, Sullivan R, Shi W. Non-disruptive, real-time analyses of the metabolic status and

viability of *Streptococcus mutans* cells in response to antimicrobial treatments. *Journal of Microbiological Methods*. 2005;**61**(2):161-170. DOI: 10.1016/j.mimet.2004.11.012

[52] Esteban Florez FL, Hiers RD, Smart K, Kreth J, Qi F, Merritt J, et al. Real-time assessment of *Streptococcus mutans* biofilm metabolism on resin composite. *Dental Materials*. 2016;**32**(10):1263-1269. DOI: 10.1016/j.dental.2016.07.010

[53] Cheng L, Weir MD, Xu HH, Antonucci JM, Kraigsley AM, Lin NJ, et al. Antibacterial amorphous calcium phosphate nanocomposites with a quaternary ammonium dimethacrylate and silver nanoparticles. *Dental Materials*. 2012;**28**(5):561-572. DOI: 10.1016/j.dental.2012.01.005

[54] Cheng L, Zhang K, Zhou CC, Weir MD, Zhou XD, Xu HH. One-year water-ageing of calcium phosphate composite containing nano-silver and quaternary ammonium to inhibit biofilms. *International Journal of Oral Science*. 2016;**8**(3):172-181. DOI: 10.1038/ijos.2016.13

[55] Li F, Weir MD, Chen J, Xu HH. Comparison of quaternary ammonium-containing with nano-silver-containing adhesive in antibacterial properties and cytotoxicity. *Dental Materials*. 2013;**29**(4):450-461. DOI: 10.1016/j.dental.2013.01.012

[56] Melo MA, Guedes SF, Xu HH, Rodrigues LK. Nanotechnology-based restorative materials for dental caries management. *Trends in Biotechnology*. 2013;**31**(8):459-467. DOI: 10.1016/j.tibitech.2013.05.010

[57] Imazato S. Bio-active restorative materials with antibacterial effects; new dimension of innovation in restorative dentistry. *Dental Materials Journal*. 2009;**28**(1):11-19. DOI: 10.4012/dmj.28.11

[58] Wang JJ, Liu F. Photoinduced graft polymerization of 2-methacryloyloxyethyl phosphorylcholine on silicone hydrogels for reducing protein adsorption. *Journal of Materials Science. Materials in Medicine*. 2011;**22**(12):2651-2657. DOI: 10.1007/s10856-011-4452-y

[59] Zhang N, Zhang K, Xie X, Dai Z, Zhao Z, Imazato S, et al. Nanostructured polymeric materials with protein-repellent and anti-caries properties for dental applications. *Nanomaterials*. 2018;**8**:393. DOI: 10.3390/nano8060393